The Wide Field Camera 3 Detectors

S.M. Baggett[1], J.W. MacKenty[1], R.A. Kimble[2], B. Hilbert[1], P. McCullough[1], T. Borders[1], A. Riess[1], H. Bushouse[1], S. Deustua[1], R.J. Hill[2], N.R. Collins[4], L. Dressel[1], M. Dulude[1], R. Foltz[2], G. Hartig[1], J. Kalirai[1], N. Pirzkal[1], V. Kozhurina-Platais[1], E. Malumuth[3], B. McLean[1], C. Pavlovsky[1], L. Petro[1], A. Rajan[1], E. Sabbi[1], A. Viana[1], T. Wheeler[1], M. Wong[1]

1. Space Telescope Science Institute 2. NASA/Goddard Space Flight Center 3. Wyle Information Systems

Introduction

WFC3 is a fourth-generation instrument installed on HST May 2009. Designed as a panchromatic camera, it features both a UVIS and an IR channel, selectable via a channel select mechanism (CSM), allowing sequential imaging.

Both detectors exhibited excellent performance during post-servicing mission orbital verification and are now in standard science operations. The following sections present some highlights as well as remaining issues being addressed.

UVIS Channel

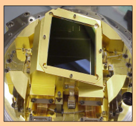

- ✓ Two e2v thinned, back-illuminated CCDs, each 2Kx4K (chips separated by ~35 pix or ~1.4")
- ✓ Range: 200-1000nm; FOV: 160"x160"
- ✓ Hermetic enclosure + vent tube to allow outgassing
- ✓ Thick-walled housing for radiation shielding
- ✓ Four 2-stage thermo-electric coolers (TECs) cool the inner radiation shield and window, a 4-stage TEC cools the CCDs to –83C
- ✓ Charge injection feature included for filling radiation-induced charge traps, contributing relatively low noise (~15e^- for ~10K e^- injected)
- ✓ Standard readout: full-frame through 4 amps (optional binning or subarrays)
- ✓ Physical / virtual serial overscans; virtual parallel overscan

IR Channel

- ✓ Hybrid HgCdTe device by Teledyne Imaging Sensors
- ✓ Thinned substrate to eliminate radiation-induced luminescence
- ✓ Hawaii-1R MUX, 1024x1024 pixels (1014x1014 active, with peripheral reference pixels to correct thermal and/or electrical drifts)
- ✓ Range: 800-1700 nm; FOV: 123"x136"
- ✓ FPA, filters, and cold stop inside cold enclosure
- ✓ Operates at 145K via 6-stage TEC (no cryogens)
- ✓ No shutter, exposures controlled electronically
- ✓ Multiaccum readout, up to 16 non-destructive reads, via 4 amps

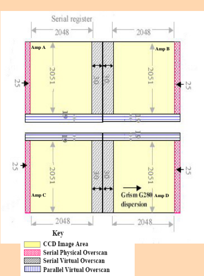

Figure 1. CCD readout configuation

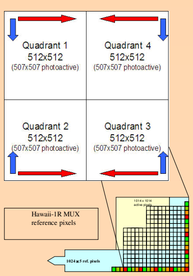

Figure 2. IR FPA readout

Further information

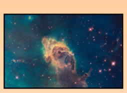

http://www.stsci.edu/hst/wfc3

http://wfc3.gsfc.nasa.gov

Also at this conference

Related talk on Friday at 10:10 -- R. Kimble et. al., "In-flight Performance of the Detectors on HST/WFC3"

Related poster -- R.J. Hill et. al., "Reciprocity Failure in 1.7um Cutoff HgCdTe Detectors"

UVIS Detectors

Quantum Efficiency and Cosmetics

The QE is high, particularly in the UV. Fig. 3 plots electrons out per photon in, which in principle includes quantum yield effects below 340nm (>1 e^-/detected photon), but these effects have been measured to be very small for these devices (~7% at 218nm and ~3% at 275nm). Cosmetics are excellent (Fig 4): <0.2% of pixels outside of +/-10% QE and <0.05% dead or bad. The vignetting at lower left is an artifact of the ground test stimulus. The wedge-shaped feature (vertex at lower right) is an expected result of reflections between the CCDs and housing windows, as AR coatings are not fully effective for such a broadband camera.

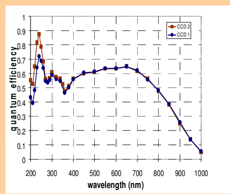

Figure 3. UVIS quantum efficiency

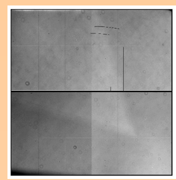

Figure 4. Flat at +/-10% stretch. Most features are stable, repeatable to < 1%.

Read noise, dark current, and linearity

These are excellent: read noise ~3 e^-/sec/pix, dark current 1-2 e^-/hr/pix (<1% of the pixels in tail >60 e^-/hr/pix) and linearity better than 5% up to 70-85K e^-.

Radiation damage – Charge transfer degradation on-orbit, taking into account the lower dark current in WFC3, is following the ACS trend observed for the 200 days after its installation in HST. Initial analysis shows that over 28 days, about 0.4-0.5% of the chip develops hot pixels (defined as >20 e^-/hr); the monthly anneals successfully repair >70%.

Crosstalk – Significant non-linear crosstalk seen in earlier detector packages was eliminated by speeding up the A/D conversion and changing the sampling time so that it no longer overlaps the previous pixel's A/D conversion process. A small amount (~7x10^{-5} to ~1x10^{-4}) remains but is linear, and thus correctable in post-readout image data processing.

Preventing hysteresis – Ground test data showed a 'bowtie' feature as well as occasional spots from images taken hours earlier, at levels ~0.1-0.2% at -83C. The DCL at GSFC reproduced a similar effect by cooling the CCDs without any illumination; furthermore, they showed that 1) a *uniform* QE deficit could be present after such cooling, 2) the chips could be pinned by a saturated flatfield, and 3) the pinning was effective for timescales of days. On-orbit, the internal lamps are used to flash the chips. Though not a bowtie, there does appear to be a QE offset after anneals, which the post-anneal pinning flat effectively neutralizes.

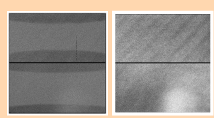

Figure 5. Ratios of internal flats. At left is the ground based 'bowtie' (~0.2% feature) and at right is the on-orbit pattern which is eradicated via the pinning exposure.

More IR Detector

Crosstalk – The IR FPA exhibits some low-level (~10^{-4}) negative crosstalk at the mirror image location of paired quadrants (more data are required to determine whether the effect is linear). Dithering may be able to help.

Cosmic rays – Some cosmic rays show both positive (CR+) and negative (CR-) components, separated by a gap. The CR- are typically 10-100x fainter than the CR+. The CR+ may be in the HgCdTe, the gap in the epoxy, and the CR- likely in the mux.

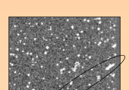

Fig 11. Extended cosmicray.

IR Detector

Quantum Efficiency and Cosmetics

The QE is excellent (Fig 7; already includes a correction for the inter-pixel capacitance effect ~13%). Cosmetically, there are sharp, high frequency features due to blemishes on the device as well as a handful of broader features, such as the small round spot of non-functional pixels at bottom, and the semi-circular area at the lower right, where QE is ~25% less than normal (Fig 8). All of these features are stable over time to better than 1%.

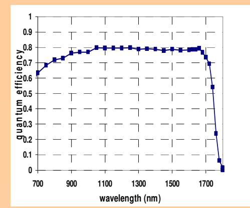

Figure 7. IR quantum efficiency

Figure 8. Flat at +/-20% stretch. Most features are stable, repeatable to < 1%.

Read noise, dark current, and linearity

On-orbit, CDS read noise is 20-22 e^-/pix RMS (up the ramp: 12.5 e^-), dark current ~0.05 e^-/sec/pix, with ~1% of the pixels in the tail (> 0.4 e^-/s/pix).

Persistence – As for most IR detectors, there are additive afterimages in WFC3, in this case, well fit by a power law $Ct^{-\alpha}$. For over-exposed spots, C=0.08-0.3 e^-/s/pix, α=1.25-1.5, and t is time; a 100xFW flat has C=0.16 e^-/s/pix and α=1.0. Persistence from signals under FW lasts <20 min; for ~100x full-well, it can take hours to decay. Dithering may help but other options are being explored.

Other afterimages – Another type of afterimage - not solely persistence - appears to be present. For example, some early data showed enhanced signal in flat-field exposures in regions that had been illuminated beyond full well shortly before. Interpreted as an additive signal, the enhancement was much larger than expected for persistence, suggesting a true sensitivity enhancement (QEH) instead. However, the enhancement was not strictly multiplicative either, ranging from <1% for signal levels below zero diode bias (the limit of the recommended operating range) to as large as 2.6% beyond that limit.The behavior has not been fully characterized, but has not been seen to exceed 1% in the nominal operating range of the detector; investigations of this behavior in the DCL with flight spare devices are ongoing.

Fig 9. At left, M81 in 1100nm; at right, ratio of a ~1000nm flat taken 40 min afterwards to a prior flat.

Rate-dependent non-linearity – Similar to the HST NICMOS instrument, the WFC3 FPA exhibits a count rate non-linearity in the sense that more counts per input photon are detected from sources with higher count rates. Since HST photometric calibration targets can be orders of magnitude (up to 10^4-10^6) brighter than some faint science targets, this becomes a significant issue. In NICMOS, the effect was 6% (at ~1100nm) and ~3% (~1600nm) for every factor of 10 change in flux. Preliminary results indicate such non-linearity in WFC3 at ~1-2%/dex . DCL tests on spare devices showed 0.4% to 1.1/dex effect. An on-orbit calibration program designed to quantify the effect is scheduled to run this observing cycle. See also Hill et al. poster at this workshop.

Fig 10. Snowballs

Snowballs – These bright, extended, transient sources, 10-30 pix in size, containing 200K-900K e^-, tend to occur near unstable pixels. The rate on the ground was ~1 snowball/2 hrs; on-orbit, preliminary results seem to indicate the rate could be ~2-3x higher. They may be due to radioactive decay within, or energetic particle interations with, the detector material. Since they mimic cosmic rays, the calibration software successfully removes them.